Joint-inversion of Soil Profile with Receiver Function and Dispersion Curve using Arrays of Seismometers

D.Calderon[1], T.Sekiguchi[1], S.Nakai[1], Z.Aguilar[2], F.Lazares[2]
[1]Department of Urban Environment System, Chiba University, 1-33 Yayoi-cho, Inage-ku, Chiba, Chiba, Japan
[2] CISMID, National University of Engineering, Rimac, Lima, Peru
email: diana_c@graduate.chiba-u.jp, tsekiguc@faculty.chiba-u.jp, nakai@faculty.chiba-u.jp
zaguilar@uni.edu.pe, f_lazares@uni.edu.pe

ABSTRACT: The soil profile estimation of Lima, the capital of Peru, is of great importance to adequately design buildings to withstand seismic activity. Particularly, the La Molina district, known for being a rapidly developing urban area, as well as having reported notable damage during past seismic events, has been studied largely. However, these studies have not explored depths greater than 50m. In this study, we intend to estimate soil profiles with depths reaching to the basement rock in La Molina. For this purpose we will apply the joint-inversion technique of dispersion curve and receiver function. The inversion of dispersion curve alone and receiver function alone is initially performed separately. The resulting inverted profiles will be used as a reference for the boundary matrix of the joint-inversion method. Our results have shown that the H/V spectrum obtained with the inverted profile is in good agreement with the observed H/V spectrum obtained with microtremor measurements. Moreover, it is in good agreement with available boring data and Ps logging profile.

KEY WORDS: Phase velocity dispersion curve; Receiver function; Joint-inversion; Shear-wave velocity profile

1 INTRODUCTION

In March 2010, the project "Enhancement in the Earthquake and Tsunami Disaster Mitigation Technology in Peru" (SATREPS) started with support of the Japan International Cooperation Agency (JICA) and the Japan Science and Technology Agency (JST).

The objective of the first stage of this project is the microzonation of Lima, the capital of Peru, which is situated on the central coast of Peru, bordered by the Pacific Ocean, in a zone of high seismic activity known as the Ring of Fire.

In this study, the soil profile estimation extending down to the seismic bedrock is carried out using the joint-inversion technique of dispersion curve and receiver functions. The target area is the La Molina district, located in a valley to the east of Lima (Figure 1).

According to Repetto et al. (1980) the La Molina district was formed by alluvial materials deposited by the ancient tributaries of the Rimac River (Quebrada Pampa Grande and Pampa Arenal). He also stated that the low area at La Molina may have been a lake in the past, and that the soils deposits in the area contain higher levels of silt and clay to depths of at least 16 m below the existing ground surface.

Historically, La Molina has reported excessive earthquake damage during the most significant earthquakes in Lima, showing a higher intensity than in central Lima; where damage tended to be lower (Stephenson et al., 2009), hence the importance of the soil profile estimation in this district.

The joint-inversion method of receiver function and dispersion curve has been often used during recent decades.. The merit of this method is the improvement in the estimation of soil profiles using the joint-inversion method when compared with stand-alone inversions.

Julia et al. (1998) mentioned that surface waves provide constraints on averages of the absolute shear velocities at different depth ranges. Ammon et al. (1990) discussed that the receiver function constrains shear velocity contrasts of interfaces located in the medium and the relative travel time of the converted waves reverberated between those interfaces.

Julia et al.(2000) mentioned that the joint-interpretation of surface wave dispersion and teleseismic P-wave receiver function seems intuitively to provide tighter constraints on the shear velocity structure than any technique individually.

2 APPLICATION OF THE JOINT INVERSION

We used data recorded in the seismic station named MOL that belongs to the CISMID accelerometer network. This station ceased operation in 2008.

2.1 Observed Receiver Function

The observed receiver function was calculated using records from four earthquakes with epicenters located about 150 km south-west of the seismic station MOL.

Figure 1 (a) shows the location of station MOL, the array EMO and the earthquakes epicenters on the soil distribution map (Cismid, 2005); while Figure 1 (b) additionally shows the location of the measurement for the MASW method conducted by Cismid (2010). Table 1 contains the information of the events used for the calculation.

These earthquakes were chosen because they have a similar incident angle, focal distance and azimuth.

The average of the receiver functions of the four earthquakes is the observed receiver function shown in Figure 2.

2.2 *Observed Dispersion Curve*

In the calculation of the observed dispersion curve, linear arrays and circular arrays of sensors (Figure 3) were measured. The method of analysis and characteristics of the arrays and sensors are discussed more in Calderon et al. (2011).

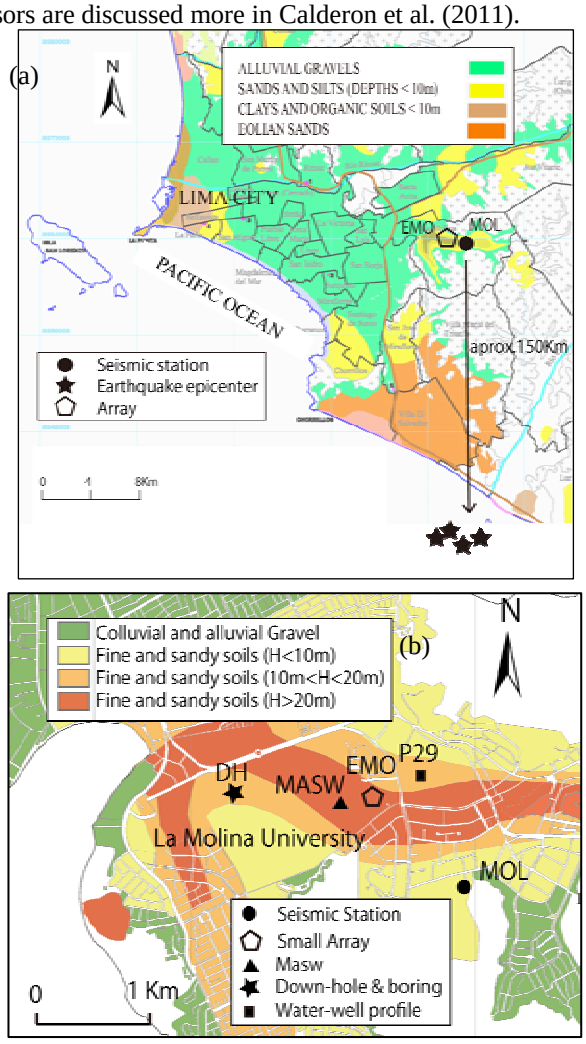

Figure 1 (a) Location of seismic station MOL, earthquakes epicenters and array EMO; (b) soil distribution map (Cismid, 2010) showing additionally MASW, down-hole, and water-well location.

Table 1. Characteristics of the seismic events used for the calculation of the observed receiver function

Date	Time	Depth (km)	ML	Inc angle (°)
2006/10/20	05:49:07	43	6.2	75.5
2006/10/26	17:54:40	42	5.8	74.7
2007/08/15	19:02:55	30	4.9	78.6
2007/08/15	20:02:38	34	5.5	77.1

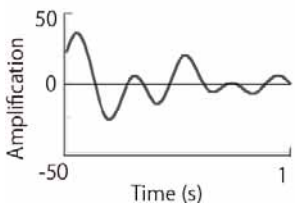

Figure 2. Averaged observed receiver function

2.3 *Inversion of Dispersion Curve alone*

In this study, as in Calderon et al. (2011), the complete curve shown in Figure 3 was used as the target for the stand-alone dispersion curve inversion process. The inversion results are shown in Figure 4.

2.4 *Inversion of Receiver Function alone*

For this inversion a boundary matrix is defined after a trial and error process. The calculated dispersion curve is shown in Figure 5 and the inverted profile is shown in Figure

2.5 *Joint-Inversion*

Based on the profiles obtained in the individual inversion process carried out in the previous section, we created a boundary matrix for the joint-inversion (Table 2).

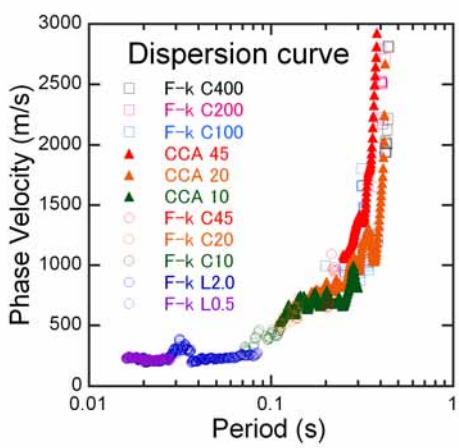

Figure 3. Observed dispersion curve

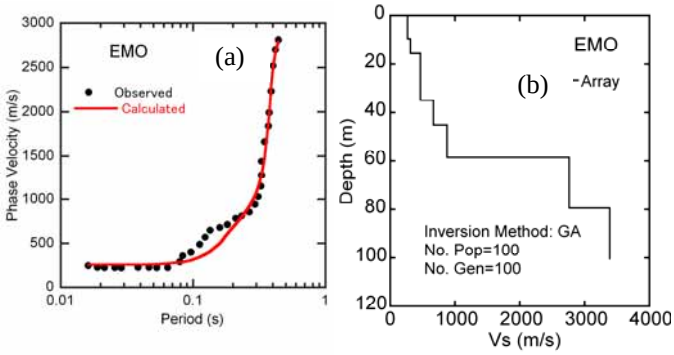

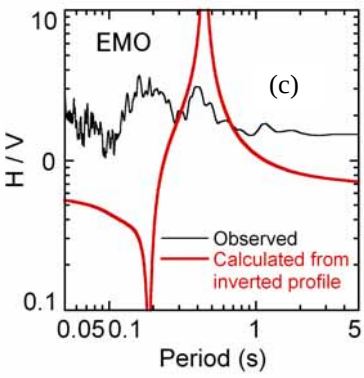

Figure 4. Inversion of dispersion curve stand-alone.(a) observed and calculated dispersion curve. (b) inverted profile (c) observed and calculated H/V spectrum

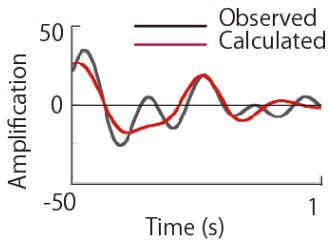

Figure 5. Calculated receiver function after the inversion

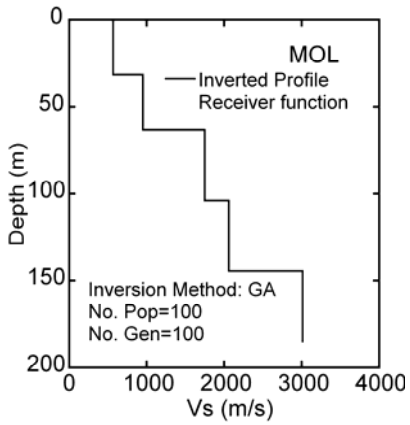

Figure 6. Inverted profile after using the inversion of receiver function alone.

For the upper layers, the boundaries were chosen based on the profile obtained by the dispersion curve inversion; and for the deep layers the boundaries were chosen based on the profile obtained by the receiver function inversion.

For the evaluation function we have followed Kurose and Yamanaka (2006).

$$\varphi_{RF} = \left(\frac{1}{N_{RF}}\right)\sum\left[\frac{R_{obs}(t_i) - R_{cal}(t_i)}{\sigma_{RF}(t_i)}\right]^2 \qquad (1)$$

$$\varphi_{ph} = \left(\frac{1}{N_{ph}}\right)\sum\left[\frac{C_{obs}(T_i) - C_{cal}(T_i)}{\sigma_{ph}(t_i)}\right]^2 \qquad (2)$$

$$\varphi = 0.5(\varphi_{ph} + \varphi_{RF}) \qquad (3)$$

where:

N_{RF} and N_{ph} are the number of data;
$\sigma_{RF}(t_i)$ and $\sigma_{ph}(t_i)$ are the standard deviations of the receiver function $R_{obs}(t_i)$ at time t_i
$C_{obs}(T_j)$ is the observed phase velocity at period T_j
φ is the objective function of the joint-inversion

Results of calculated receiver function, dispersion curve, and the inverted profiles are shown in Figure 7.
Finally the profile data is used to calculate the H/V spectrum (Figure 8).

Table 2. Boundary matrix for the Joint-inversion

Vs (m/s)	H(m)
[150-300]	[1-10]
[300-500]	[1-10]
[500-1000]	[5-20]
[500-1000]	[5-20]
[700-1200]	[10-30]
[1500-1800]	[20-40]
[2000-2300]	[20-40]
[3000-3300]	-

3 AVAILABLE BORING DATA AND DOWN-HOLE

A very deep water-well logging down to the bedrock was conducted by the Water and Sewerage Company of Lima. This data was collected by Cismid (2010) and identified as P29. The soil column is shown in Figure 9. In this profile the rock is found at 130m.

The only down-hole data available in this area was from a measurement carried out after the October, 1974 Lima's earthquake, the exact location of this logging is unknown but it is about 100m from the old location of station MOL(Repetto, 1980). A boring data from this place is also available. Both the down-hole profile and the soil column are identified as DH and are shown in Figure 10(a) and 10(b) respectively.

4 DISCUSSION

4.1 Observed Dispersion Curve

The observed phase velocity dispersion curve (Figure 3) shows a shoulder for periods from 0.1 to 0.3 s. This behavior generally is caused when a layer of higher velocity is overlying a layer of lower shear velocity. In our case, after the inversion, the calculated dispersion curve does not fit the observed one in the period range where the shoulder appears. Therefore, the real values of velocities in this range of periods may be underestimated.

Another special characteristic of the observed dispersion curve is the steep slope for the period range from 0.25 to 0.45 s. The velocities in this range are more scattered than for shorter periods. According to Kurose and Yamanaka (2006), this is a result of the small amplitudes of long-period microtremors.

Yamanaka et al. (1995) pointed out the lower resolution in deep structure after inverting phase velocities for periods up to 5 seconds in Tokyo, Japan. In the case of Lima, the soils are more rigid than in Japan; thus the limit period is expected to be shorter; for La Molina the limit could be considered 0.3 s.

However, in order to verify the resolution of the deep structure obtained by inverting the dispersion curve alone, observed phase velocities up to 0.3 s were taken. The resulting velocity profile is shown in Figure 4(b). Here the basement rock is found at 60 m depth. Later we compare the profiles with the joint-inversion and verify the resolution.

4.2 Observed Receiver Function

Although the quantity of seismic records used for the calculation of the averaged observed receiver function is small,

the similarity of the characteristics of the earthquakes led us to an acceptable receiver function.

When performing the inversion of the receiver function alone, we can see in Figure 5 the correlation in the first and third peaks, but not in the second peak. This is likely due to the problems inherent in using the inversion receiver function alone, that is, that low resolution fails to accurately estimate the shallow layers.

4.3 Joint-inverted Profile

For the joint-inversion the observed dispersion curve was limited to 0.3s; this is because it is expected that the deep structure is constrained by the receiver function. Despite the calculated dispersion curve not fitting well with the observed curve for periods up to 0.1 s (which can cause a high or low estimation of the shear velocity in shallow layers); the H/V spectrum of the inverted profile shows a good agreement with the observed H/V spectrum calculated from one point microtremor measurements. These spectra show more than one peak, which accounts for the diverse soil layers as seen in the profile.

4.4 Comparison with available boring data and down-hole

When comparing the down-hole data with the inverted profile (Figure 7(c) and (d)) we can see a good agreement for the upper layers.

The other data we have to compare is the water-well logging, which indicates that the rock is at 130m. When looking at this depth in the inverted profile estimated with the joint-inversion (Figure 7(d)); we found that the bedrock is at about 110m; verifying this the resolution of the inverted profile.

4.5 Influence on the Distance between the Seismometer Station and the Array Location.

The array EMO was carried out on the campus of La Molina University, which is about 1 km distance from the MOL station (Figure 1(b)).

La Molina district is in a valley where the depth to the bedrock is variable over short distances, and that is the reason why we want to verify the influence of the separation distance between EMO and MOL when applying the joint-inversion method.

In Stephenson et al. (2009) it is mentioned that the MOL station is over a coarse gravel substrate, and the bedrock is 20-30m depth. The EMO array, on the contrary, is located on the University campus, in the middle of a valley.

The difference in the shallow soils for these two places could account for the misfit of the first phase in the calculated receiver function (Figure 7(a)). However, since the receiver function places constraints on deep structure, which is homogeneous in both places, for a depth of more than 100m, and the dispersion curve controls the shallow structure, the final inverted profile can be considered valid for the location of the seismometer array EMO. The agreement in the H/V spectra, boring data, and down-hole logging verifies this statement.

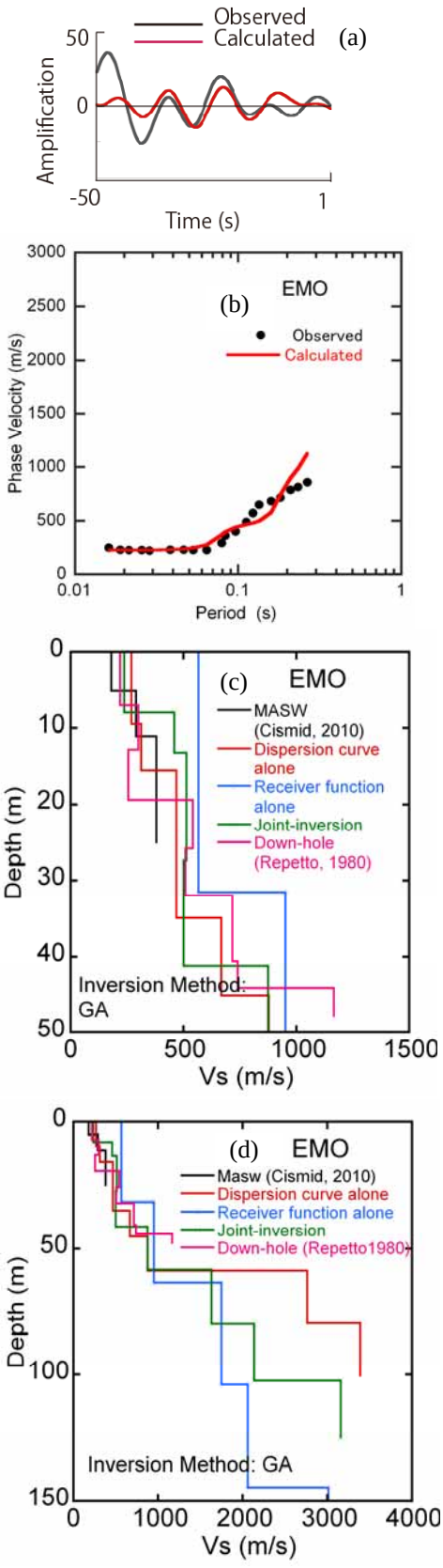

Figure 7(a) Observed and calculated receiver function. (b) Observed and calculated dispersion curve. (c); and (d) Comparison of soil profiles obtained by stand alone methods, joint-inversion method and MASW for the first 50m and 150m respectively.

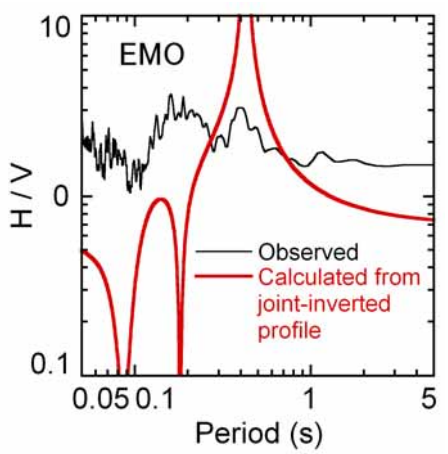

Figure 8. Observed and calculated H/V spectrum from the joint-inverted profile

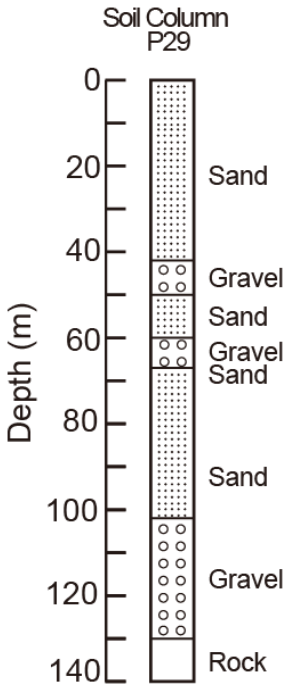

Figure 9. Water-well logging (data collected by Cismid, 2010 from the Water and Sewerage Company of Lima)

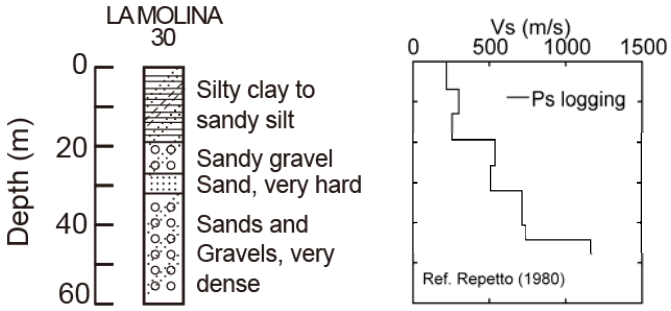

(a) (b)

Figure 10(a) and (b). Boring data and down-hole profile respectively (Repetto, 1980)

4. CONCLUSIONS

The application of the joint-inversion method of receiver function and dispersion curve led us to the next conclusions:

- For the array in La Molina (EMO), the largest period in the phase velocity curve where we can expect acceptable results, is about 0.3s.
- The inverted profile estimate with the joint-inversion method can be considered representative for the location of the EMO array.
- Future plans for the SATREPS project include installing a seismometer near the area where the EMO array was conducted. Using the seismic records from this station, a verification of the profile presented in this study is recommended as a future goal.

ACKNOWLEDGMENTS

We would like to express our thanks to the people at CISMID, especially to Eng. Selene Quispe, for her assistance in providing the data; and to the research assistants for their help in performing the measurements.

REFERENCES

[1] Ammon, C.J., Randall, G.E.&Zandt, G., 1990. On the nonuniqueness of receiver function inversions, *J. geophys. Res.*, 95, 15 303-15 318.

[2] Calderon, D., Sekiguchi, T., Aguilar, Z., Lazares, F., Nakai, S., 2011. Dynamic Characteristics of the Surface Soils in Lima, Peru, 8th International Conference in Urban Earthquake Engineering. March 7-8, 2011, Tokyo Institute of Technology, Tokyo, Japan. (submitted)

[3] Cismid, 2005. Study of the Vulnerability and Seismic Risk in 42 districts of Lima and Callao. Japan - Peru Center for Seismic research and Disaster Mitigation, National University of Engineering, Lima, Peru. *(in Spanish)*

[4] Cismid, 2010. Microzonificacion Sismica del distrito de La Molina. Japan - Peru Center for Seismic research and Disaster Mitigation, National University of Engineering, Lima, Peru. *(in Spanish)*

[5] Julia, J., Vila, J.&Macia, R., 1998. The receiver structure beneath the Ebro basin, Iberian Peninsula, *Bull. Seism. Soc. Am.*, 88, 1538-1547.

[6] Julia, J., Ammon, C.J., Herr,ann, R.B., Correig, A.M., 2000. Joint inversion of receiver function and surface wave dispersion observation. *Geophys. J. Int.*, 143, 99- 112.

[7] Kurose, T., Yamanaka, H., 2006. Joint inversion of receiver function and surface-wave phase velocity for estimation of shear-wave velocity of sedimentary layers. *Exploration Geophysics*, 37, 93-101.

[8] Repetto, P., Arango, I., Seed, H.B., 1980. Influence in site characteristics on building damage during the October 3, 1974 Lima earthquake, Report-Earthquake Engineering Research Center, College of Engineering University of California, NTIS, 80-41

[9] Stephenson, W.R., Benites, R.A., Davenport, P.N., 2009. Localised coherent response of the La Molina basin (Lima, Peru) to earthquakes, and future approaches suggested by Parkway basin (New Zealand) experience. *Soil dynamics and Earthquakes Engineering*, 29, 1347-1357.

[10] Yamanaka, H., Furuya, S., Nozawa, T., Sasaki, T., and Takai, T., 1995. Array measurements of long-period microtremors in the Kanto Plain-Estimation of S-wave velocity structure at Koto-: *Journal of Structural and Construction Engineering, Architectural Institute of Japan*, 478, 99-105.